Article:
Johnson, M, Al-Dirawi, KH, Bentham, E et al. (2 more authors) (2021) A non-adiabatic model for jacketed agitated batch reactors experiencing thermal losses. Industrial and Engineering Chemistry Research, 60 (3). pp. 1316-1325. ISSN 0888-5885

https://doi.org/10.1021/acs.iecr.0c05133

A non-adiabatic model for jacketed agitated batch reactors experiencing thermal losses

Michael Johnson,*,†,‡ Karrar H. Al-Dirawi,† Erik Bentham,† Tariq Mahmud,† and Peter J. Heggs†

†*School of Chemical and Process Engineering, University of Leeds, Leeds, LS2 9JT*

‡*Current address: CEA, DES, IRESNE, DTN, SMTA, LEAG, Cadarache, 13115 Saint-Paul-lez-Durance, France*

E-mail: Michael.Johnson@cea.fr

Abstract

Accurate modeling of process temperatures within jacketed batch reactors has the potential to mitigate the risk of thermal runaways and enhance process control. A non-adiabatic heat transfer model is derived for the investigation of heat transfer in laboratory to pilot scale reactors of 0.5–40 L. By accounting for heat removed from the process by a total condenser, and losses through the process lid, the model is able to predict process temperature profiles within the uncertainty limits of the experimental measurements. Heat losses from the outer jacket wall had a negligible impact on the evolution of process temperature but may contribute significantly to utility costs. Jacket duty measurements implied greater heat accumulation within the reactor vessel than anticipated, equivalent to $\sim 60\,\%$ of that in the process fluid at 40 L scale. This raises the potential for heat transfer coefficients to be systematically under-estimated by adiabatic models, particularly at laboratory to pilot scale.

1 Introduction

The capacity to accurately predict the temperature inside jacketed batch reactors, potentially avoiding the need for *in situ* temperature monitoring on the process side, could incur significant benefits.[1–4] Such a model could be used to precisely optimize subcooling conditions for batch cooling crystallisation[5] without extensive experimentation, or to pre-emptively avoid operating conditions for exothermic reactions vulnerable to dangerous thermal runaways.[6–8] Alternatively, an improved understanding of the thermal response of reactors to changes in the jacket duty could enable greatly enhanced temperature control on the process-side, minimizing batch times while limiting the *overshoot*[3] or instability[9] in process temperature. A typical feedback-control system[10] may use process-side temperature monitoring to manipulate the temperature and/or flow rate of the thermal fluid in the jacket. However, reactors may exhibit significant inertia in their thermal response[1,4] as the jacket fluid must raise, or lower, the temperature of the vessel before heat can accumulate in, or dissipate from, the process-fluid. The cumulative times for communication of *in situ* temperature data, the requisite time to adjust the heating or cooling duty, combined with the thermal inertia of the vessel, the jacket, the pipework and the thermoregulator can entail a sluggish response and departure from the designed operating conditions. The responsiveness of the control system could be greatly improved through predictive, feed-forward or adaptive[11,12] control approaches combined with a more comprehensive and precise characterization of the reactor system.

Commonly employed lumped-parameter heat transfer models[13,14] derive from a simplified description of the reactor energy balance, employing assumptions such as perfect mixing on the process side, negligible residence time in the thermal jacket, instantaneous thermal response times, use of an overall heat transfer coefficient (OHTC), U, and perfect insulation of the process vessel and thermal jacket.[15] Sophisticated on-line control systems for batch reactors,[3,16] and heat of reaction calorimeters,[17] still regularly employ such assumptions in their heat transfer models. Advancements in computational power invite the possibility

Nomenclature

A	heat transfer area
E	thermal effectiveness
E_{mod}	modified thermal effectiveness
Q	quantity of heat transferred
T	temperature
Φ	Phi-factor, or thermal inertia
α	heat transfer film coefficient
α_0	free convection film coefficient
c_p	specific heat capacity
t	time
D	diameter
H	height
M	mass
U	overall heat transfer coefficient
δ	thickness
$\dot{M}$	mass flow
$\dot{Q}$	heat flow
u	measurement uncertainty
x	position along the length of the jacket

Superscripts

$\dot{}$	time derivative
$\tilde{}$	dimensionless

Subscripts

0	initial condition, $t = 0$
1	inlet
2	outlet
∞	ambient
C	cooling
c	condenser
d	dished portion of the reactor vessel
H	heating
j	jacket
$jloss$	jacket losses
p	process
$ploss$	process losses
s	source (generation/consumption)
set	target
w	wall

of a more precise representation of jacketed batch reactors, addressing the more onerous assumptions of the lumped model, without excessive computation times.[4]

The assumption employed by the classical adiabatic model, that the reactor experiences negligible thermal losses and thus all heat transferred from the jacket accumulates in the process fluid, has been shown to hinder the accurate prediction of process temperature profiles, particularly at laboratory scale,[13,18] and merits a revision to the energy balance. Four avenues for thermal losses should be considered. The flow of the thermal fluid through the jacket will experience heat loss to the ambient surroundings due to free convection

and thermal radiation at the outer jacket wall. The vapour in the vessel ullage will be in equilibrium with the process fluid and so will condense on the cool internal surface of the vessel above the fluid level resulting in heat loss to the ambient surroundings. Likewise, any vapours entering an overhead condenser (which are, on occasion, necessary to maintain a near constant liquid volume in the reactor) will remove heat from the process. In addition to the thermal losses to the ambient surroundings, the thermal jacket duty must raise/lower the temperature of the total mass of the equipment (including the process and jacket walls and the agitator) as well as that of the process fluid. Heat accumulation within the equipment can correspond to a significant portion of the total thermal jacket duty, often resulting in a sluggish control response and undesirable overshoot of the process set temperature. Failure to account for all these thermal losses has resulted in studies reporting distinct OHTCs for heating and cooling regimes,[19,20] since thermal losses retard heat accumulation and accelerate dissipation from the process. Consequently, many OHTC values quoted in the literature, ascertained using the assumptions employed by these lumped adiabatic models, are likely to pertain to specific temperature plans and ambient conditions. Furthermore, the sizing of external equipment[21] (heat exchangers or thermoregulators) to supply the thermal duty for heating operation may be underestimated (or overestimated for cooling operation) on the basis of lumped, adiabatic models.

An ordinary differential equation (ODE) model proposed in a previous work by the current authors[18] demonstrated improved performance by considering the influence of thermal losses through the reactor lid, but stopped short of presenting an entirely non-adiabatic model inclusive of thermal losses from the outer jacket wall and heat removed from the process by an overhead total condenser. This study presents the derivation of a novel, non-adiabatic model, which will be used to investigate experimental data obtained from laboratory to pilot scale jacketed agitated batch reactors of sizes 0.5, 5 and 40 L. The heat transfer model will be used to explore the significance of the jacket-side thermal losses and the impact of the thermal mass of the reactor vessel and components on the heating or cooling duty and the

total energy consumption during experimentation.

2 The non-adiabatic heat transfer model

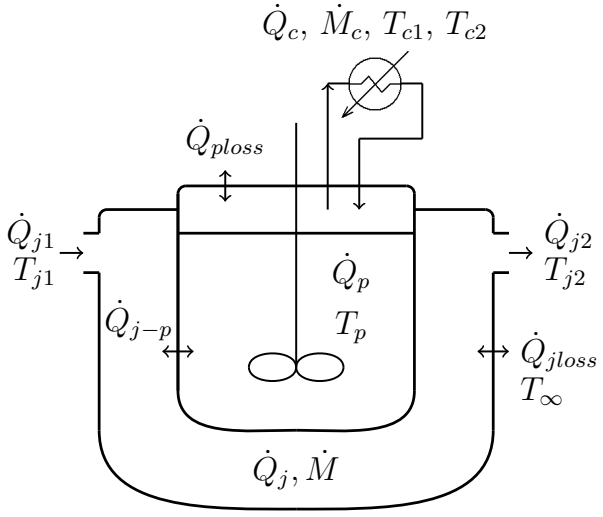

Figure 1: Schematic of heat transfer processes in a non-adiabatic jacketed batch reactor experiencing thermal losses to its surroundings and with a total condenser on the process-side.

A schematic of a jacketed batch reactor, experiencing thermal losses at the outer jacket wall and through the reactor lid, and with a total condenser to maintain a constant liquid volume on the process side, is presented in Figure 1. Various rates of heat transfer are identified in the schematic, the total rate of heat transfer from the jacket, calculated from the heat flows at the inlet and outlet, $\dot{Q}_j = \dot{Q}_{j2} - \dot{Q}_{j1}$, the rates of thermal loss from the outer jacket wall, $\dot{Q}_{jloss}$, and direct from the process side, $\dot{Q}_{ploss}$, the rate of heat transfer across the wall between the jacket and process, $\dot{Q}_{j-p}$, the condenser duty, $\dot{Q}_c$, and the rate of heat change in the process fluid, $\dot{Q}_p$. Additional sources of heat generation within the process, including heats of reaction, crystallisation or mixing, along with thermal inputs from the mechanical work of the impeller, are denoted $\dot{Q}_s$, but will not be significant for the purpose of characterizing the heat transfer behavior of the reactor systems in this study (an inert process fluid will be used to focus purely on the heat exchange processes and the

thermal input of the impeller can be considered negligible in this case). In the absence of heat generation within the process, the rate of heat change in the process fluid, and thus the evolution of process temperature, can be derived as a function of time from the initial process temperature, $T_p(0)$, various *ex situ* temperature measurements and flows, the total thermal mass, $\sum_{n=1}^{N}(Mc_p)_n$, and three products (OHTCA) of OHTCs and heat transfer areas, A, as summarized in eq. (1):

$$T_p(t) = f\left(\begin{array}{l} T_p(0), T_{j1}(t), T_\infty(t), T_{c1}(t), T_{c2}(t), (UA)_p, \\ (UA)_{jloss}, (UA)_{ploss}, \dot{M}_j, \dot{M}_c, \sum_{n=1}^{N}(Mc_p)_n \end{array}\right) \tag{1}$$

where $(UA)_p$ is the OHTCA for heat transfer from the jacked to the process, and $(UA)_{ploss}$ and $(UA)_{jloss}$ are OHTCAs for the process and jacket side thermal losses. The thermal mass term, $\sum_{n=1}^{N}(Mc_p)_n$, comprises the mass and specific heat capacity products of the reactor vessel and its constituent parts as well as that of the process fluid. In reaction calorimetry, the ratio of this augmented thermal mass, or thermal inertia, to that of the process fluid alone is labeled the Phi-factor, Φ:[22,23]

$$\Phi = \frac{\sum_{n=1}^{N}(Mc_p)_n}{(Mc_p)_p} \tag{2}$$

The Phi-factor is commonly assumed to approximate unity, 1–1.05 ,[22] at process scale (depending on the reactor construction materials), but is likely to be significantly greater for laboratory to pilot scale reactors and calorimeters (unless specifically engineered to minimize the reactor's thermal inertia[22]).

The non-adiabatic ODE model is presented in eq. (3). The complete step-wise derivation is provided in the supporting information (SI).

$$\sum_{n=1}^{N}(Mc_p)_n\frac{dT_p}{dt} = kT_{j1} - \left(\frac{k+(UA)_{jloss}}{(1+(\tilde{UA}))}+(UA)_{ploss}\right)T_p + \left(\frac{(UA)_{jloss}-(\tilde{UA})k}{(1+(\tilde{UA}))}+(UA)_{ploss}\right)T_\infty - (\dot{M}c_p)_c(T_{c2}-T_{c1})+\dot{Q}_s \tag{3}$$

Here, the recurring parameter k represents $k = \frac{E_{mod}(\dot{M}c_p)_j}{(1+(\tilde{UA}))}$, the modified thermal effectiveness is given by $E_{mod} = 1 - exp\left(-\frac{(UA)_p+(UA)_{jloss}}{(\dot{M}c_p)_j}\right)$ and a dimensionless OHTCA denotes $(\tilde{UA}) = \frac{(UA)_{jloss}}{(UA)_p}$. This ODE heat transfer model simplifies under many mildly different reactor configurations and commonly applied assumptions. In the absence of the condenser, $\dot{M}_c \to 0$, no reaction heat, $\dot{Q}_s \to 0$, and for a well-insulated jacket, $(UA)_{jloss}\,\&\,(\tilde{UA}) \to 0$, eq. (3) reduces to the two coefficient *semi-adiabatic* model previously presented in Johnson et al.[18]:

$$\sum_{n=1}^{N}(Mc_p)_n\frac{dT_p}{dt} = E(\dot{M}c_p)_j(T_{j1}-T_p) + (UA)_{ploss}(T_\infty - T_p) \tag{4}$$

where $E = 1 - exp\left(-\frac{(UA)_p}{(\dot{M}c_p)_j}\right)$. If the process lid is perfectly insulated ($(UA)_{ploss} \to 0$), eq. (4) reduces further to the classical adiabatic approach. Returning to the non-adiabatic model, the capacity to accurately predict the evolution of the total thermal duty of the reactor jacket represents an additional, significant measure of the model performance,[9] alongside predictions of the evolution in process temperature. A complete model should estimate the total energy consumption of operation, and thus the utility costs, in addition to the accumulation and dissipation of heat in the process fluid. The jacket duty can be calculated from the parameters listed in eq. (1) using the relationship in eq. (5):

$$-\dot{Q}_j = k\left(\left(1 + (\tilde{UA})\right)T_{j1} - T_p - (\tilde{UA})T_\infty\right) \tag{5}$$

Identities and relationships for all of the rates of heat transfer identified in Figure 1 are defined, in terms of the input parameters listed in eq. (1), in Table 1.

2.1 Numerical solution

Numerical solutions to eq. (3) are acquired using Heun's method, with a time interval of 1 s. For the purpose of assessing the rates of heat transfer from the jacket to the process, the thermal losses from the jacket and the process lid, and the heat removal by the condenser, an inert fluid will be used on the process side. Consequently, there is no process side heat generation or dissipation, $\dot{Q}_s \to 0$, and the physical properties of the process fluid will not evolve substantially during experimentation and may be approximated as constants. Under typical reactor operation, the heat transfer model will be coupled with the reaction kinetics, dictating evolution in reagent concentrations, $\frac{dC_A}{dt}$,[24,25] and the change in thermophysical properties of the reaction mixture as a function of conversion. The reaction kinetics will likely contain an Arrhenius term dictating the reaction rate to be an exponential function of process temperature, and thus additional care must be taken to ensure that the time step is sufficiently small, and the chosen numerical model sufficiently robust, to avoid escalating numerical errors and instability. Similarly, for operations involving phase changes or polymerization[26] on the process side, the physical properties and the total reactor thermal mass may evolve significantly with time and should be updated at each iteration of the numerical loop. Full characterization of the reactor system requires optimization of the three OHTCAs and the thermal mass term (or Φ) in eq. (3) to best replicate the experimentally observed evolution in process temperature and jacket duty.

Table 1: Correlations for the various rates of heat transfer identified in Figure 1

Property	Identity	Equation
$\dot{Q}_j$	$\int_0^L (\dot{M}c_p)_j \frac{dT_j(x)}{dx}\, dx$	$-k\left((1+(\tilde{UA}))T_{j1} - T_p - (\tilde{UA})T_\infty\right)$
$\dot{Q}_{j-p}$	$\int_0^L (UA')_p(T_j(x) - T_p)\, dx$	$kT_{j1} - \frac{(UA)_{jloss}+k}{(1+(\tilde{UA}))}T_p - \frac{k(UA)-(\tilde{UA})_{jloss}}{(1+(\tilde{UA}))}T_\infty$
$\dot{Q}_{jloss}$	$\int_0^L (UA')_{jloss}(T_j(x) - T_\infty)\, dx$	$k(\tilde{UA})T_{j1} + \frac{(UA)_{jloss}-k(\tilde{UA})}{1+(\tilde{UA})}T_p - \frac{k(\tilde{UA})^2+(UA)_{jloss}}{1+(\tilde{UA})}T_\infty$
$\dot{Q}_p$	$\sum_{n=1}^N (Mc_p)_n \frac{dT_p}{dt}$	$kT_{j1} - \left(\frac{k+(UA)_{jloss}}{(1+(\tilde{UA}))} + (UA)_{ploss}\right)T_p +$ $\left(\frac{(UA)_{jloss}-(\tilde{UA})k}{(1+(\tilde{UA}))} + (UA)_{ploss}\right)T_\infty -$ $(\dot{M}c_p)_c(T_{c1} - T_{c2}) + \dot{Q}_s$
$\dot{Q}_{ploss}$	$(UA)_{ploss}(T_p - T_\infty)$	$(UA)_{ploss}(T_p - T_\infty)$
$\dot{Q}_c$	$(\dot{M}c_p)_c(T_{c2} - T_{c1})$	$(\dot{M}c_p)_c(T_{c2} - T_{c1})$

3 Materials and methods

Heat transfer experiments were conducted at 0.5, 5 and 40 L scales. A schematic of the experimental configuration is presented in Figure 2a.[18] The total condenser shown in Figure 2a was used only during the pilot scale, 40 L, experiments. A thermoregulator was used to supply a thermal fluid to the reactor jacket in order to heat and cool water on the process side. A Huber Unistat 380 HT thermoregulator ($\dot{Q}_H = 2.65\,\text{kW}$ and $\dot{Q}_C(T = 20\,^\circ\text{C}) = 1.3\,\text{kW}$) was used for the 0.5–5 L reactors, while a larger Huber Unistat 510 ($\dot{Q}_H = 6\,\text{kW}$ and $\dot{Q}_C(T > 0\,^\circ\text{C}) = 5.6\,\text{kW}$) was used for the 40 L reactor.

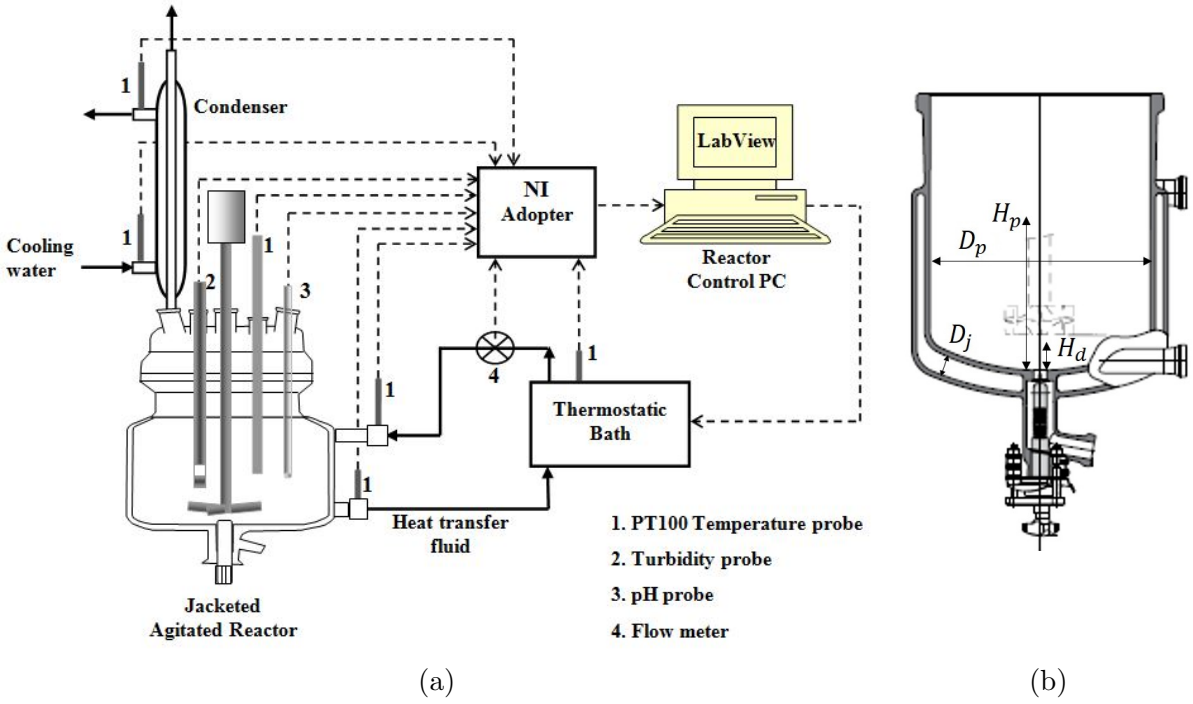

Figure 2: Schematics of (a) the experimental facility configured for the assessment of heat transfer performance[Reprinted with permission from Johnson, Heggs and Mahmud,[18] Copyright (2016) American Chemical Society] and (b) the reactor geometry [Reprinted and adapted with permission from DDPS Limited,[27] Copyright (2020) De Dietrich Process Systems GmbH.].

The heat transfer fluid on the jacket side was a triethoxysilane-based oil, DW-Therm (Radleys, U.K.). The thermoregulators were controlled using LabView software at an adjacent computer to achieve the required jacket inlet temperature profile. A heating-cooling

cycle was employed at the 0.5–5 L scales, while a simple heating ramp was used at 40 L scale. The 0.5 and 5 L experiments were controlled such that the process temperature should follow a set temperature, T_{set}, profile (process-control mode), while the 40 L experiment was controlled such that the jacket inlet temperature follows a set temperature profile (jacket-control mode). A schematic of the reactor vessels is presented in Figure 2b, and the geometric specifications of the 0.5–5 L reactors (Radleys, UK) and 40 L reactor (DDPS Limited), are provided in Table 2.

Table 2: Reactor dimensions and thermal parameters for the three experimental scales.

Reactor	1	2	3
Manufacturer	Radleys	Radleys	DDPS
Capacity (L)	0.5	5	50
Filled volume (L)	0.5	5	40
D_p (mm)	85	180	450
H_p (mm)	96	209	292
H_d (mm)	15	25	84
D_j (mm)	12	25	21
δ_{pw} (mm)	3	5	6
δ_{jw} (mm)	2.5	4	5
(Mc_p) (kJ K^{-1})	2.04	20.4	163
$\sum_{n=1}^{N}(Mc_p)_n$ (kJ K^{-1})	2.47	23.2	175
Φ	1.20	1.14	1.08
$(\dot{M}c_p)_j$ (kJ K^{-1} s^{-1})	0.231	0.180	0.882
A_p (10^{-3} m^2)	28.0	131	475
A_{ploss} (10^{-3} m^2)	5.67	25.5	159
A_{jloss} (10^{-3} m^2)	58.1	268	748

In line PT-100 temperature probes, with an uncertainty of ±0.3 K at 0 °C, were used to record process temperatures at the jacket inlet and outlet, the condenser inlet and outlet and the ambient temperature. The process temperature was monitored using a PTFE PT-100 temperature probe, with an uncertainty of ±0.15 K at 0 °C, and the flow rate in the jacket was monitored to ±1 % accuracy using a positive displacement flow meter (Caché Instrumentation Ltd., UK). Experimental measurements were logged at 1 Hz frequency during the 0.5–5 L tests and 0.03 Hz during the 40 L test by the LabView software. Ambient temperature measurements were monitored 0.5 m from the reactor vessel, under the same

fume hood. The ambient temperature was not recorded during the 40 L scale experiment and was assumed to remain constant at 20 °C throughout the experiment.

4 Results and discussion

Experimental temperature data acquired at the three process scales are presented in Figure 3. The thermoregulator demonstrates a better aptitude to precisely control the jacket inlet temperature during the 40 L experiment, operated in jacket-control mode, than it controls the process temperature during the smaller scale experiments, operated in process-control mode. This illustrates the limitations of feedback control algorithms driven by real-time, *in situ* process temperature measurements, due to the lag in responsiveness caused by the thermal inertia of the reactor system.[1,23] This inertia in process temperature response becomes more pronounced with increasing scale due to the increased thermal mass of the reactor and its contents, resulting in increased departure from the set temperature profile during the 5 L experiment, as compared with the 0.5 L test. At the end of the heating cycle of the 5 L experiment, the process temperature overshoots the set temperature by 7 °C. For certain pharmaceutical or biological applications, for instance, requiring precise control of the process conditions, an overshoot of the design operating temperature by this magnitude could be sufficient to ruin the batch.

During the 40 L scale test, the process temperature asymptotes at a steady-state temperature around 0.9 K below the jacket inlet and outlet temperatures, demonstrating the influence of thermal losses from the process side,[18] including both the thermal losses from the reactor lid and the heat removed by the condenser. Given sufficient batch times, the difference between jacket inlet and process temperatures will exponentially decay to zero for an adiabatic reactor, and thus a positive OHTCA for process losses is a prerequisite to accurately predict the evolution of process temperature.[18] The thermal losses are also observed through the mild rise in ambient temperature in Figure 3a, measured 0.5 m from

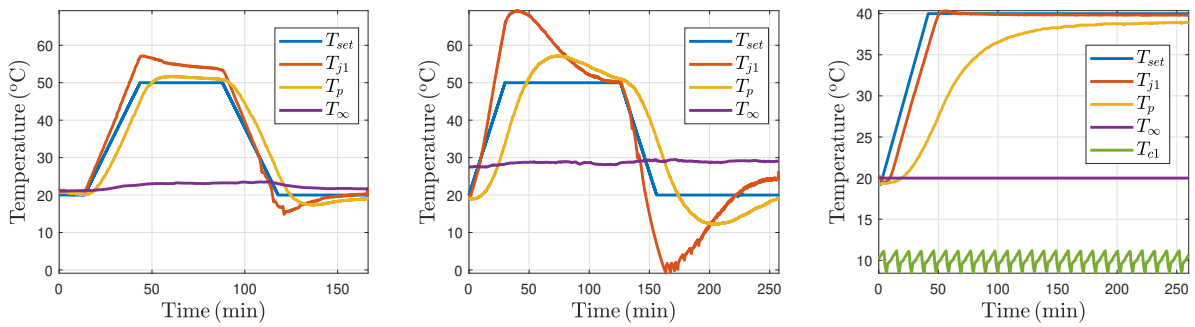

Figure 3: The evolution of set temperature, process, jacket inlet, ambient and condenser inlet temperatures during heating/cooling experiments in (a) 0.5 L, (b) 5 L and (c) 40 L jacketed batch reactors

the 0.5 L reactor, while the process and jacket temperatures are elevated. In addition to the 0.15–0.3 K uncertainties in the temperature measurements, the ambient temperature measurements were found to be sensitive to the probe location, which presents an additional challenge for estimating the thermal losses.

4.1 Modeling process temperature under semi-adiabatic conditions (a perfectly insulated outer jacket wall)

Initially, in order to model the evolution of process temperature at the three experimental scales, the semi-adiabatic, or perfectly insulated thermal jacket ($(UA)_{jloss} \rightarrow 0$), assumption was considered. Table 3 lists the estimated thermal mass of the three reactor systems and the OHTCAs for heat transfer to the process and process losses used to predict the response of the temperatures on the process-side. The corresponding predictions of the ODE model are presented in Figure 4.

For significant portions of each test, the predicted process temperature profiles very closely mirror the experimental measurements at all three experimental scales, with the departure from the experimental data comparable to the uncertainty inherent to the PT-100 temperature probe measurements. The model performs less well at the start and end of the

Table 3: Model parameters used in the predictions of the process temperature responses for a semi-adiabatic assumption (perfectly insulated thermal jacket).

Volume (L)	$\sum_{n=1}^{N}(Mc_p)_n$ (kJ K^{-1})	Φ	$(UA)_p$ (W K^{-1})	$(UA)_{ploss}$ (W K^{-1})	$(UA)_{jloss}$ (W K^{-1})	$\frac{(UA)_p}{(UA)_{ploss}}$
0.5	2.5	1.20	5.07	0.58	0	8.7
5	23	1.14	13.4	0.9	0	14.9
40	175	1.08	89	3.5	0	25.4

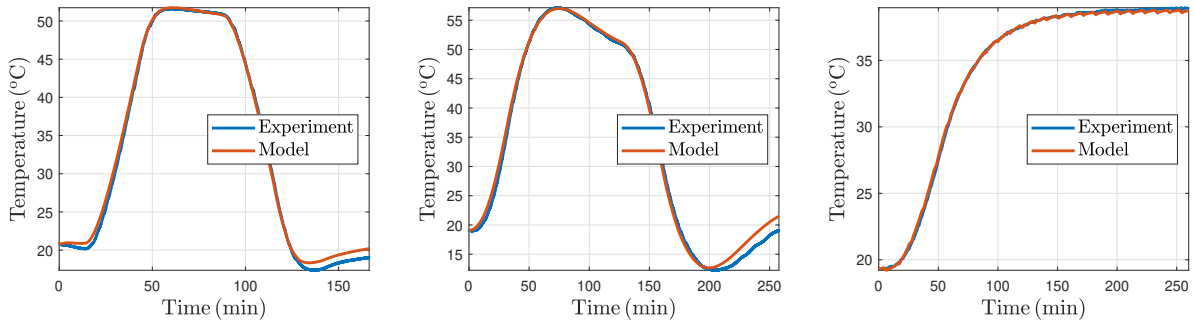

Figure 4: Profiles of the experimental process temperatures with corresponding predictions using the ODE model, assuming a perfectly insulated outer jacket wall (eq. (4)), at (a) 0.5, (b) 5 and (c) 40 L scales

0.5 and 5 L experiments when the process temperature is close to the ambient temperature due to the uncertainties in ambient temperature measurements. The fact that the predicted process temperatures equilibriate at a temperature above the *in situ* measurements likely indicates that the ambient temperature measurements were artificially high due to the temperature probe being placed too close to the reactor. Thus, the largest departure from the experimental data could be diminished by simply monitoring the ambient temperature at multiple locations.

The promising performance of the semi-adiabatic model would appear to indicate that the thermal losses from the outer jacket wall do not particularly influence the rate of heat accumulation on, and dissipation from, the process side. Since the flow rate in the thermal jacket is typically high and the residence time in the jacket and temperature drop along the length of the jacket are low, the driving force for heat transfer from the jacket to the process, $T_j(x) - T_p$, will be virtually uniform across the inner wall of the jacket and is unlikely to be

heavily influenced by the magnitude of the thermal losses at the outer jacket wall. However, the jacket losses will contribute the total duty of the thermal jacket, $-\dot{Q}_j = \dot{Q}_{j-p} + \dot{Q}_{jloss}$. If the thermal losses correspond to a significant portion of the thermoregulator's heating duty then this could compromise the capacity of the thermoregulator to achieve the desired jacket inlet temperature profile. It is therefore important to consider the duty of the thermal jacket, in addition to the evolution in process temperature, when assessing the heat transfer model performance.

A major obstacle to assessment of the thermal duty of the jacket is that the low residence time in the jacket necessitates a small temperature drop along the length of the jacket, which is often comparable in magnitude to the $\pm 0.3\,\mathrm{K}$ uncertainty in the temperature measurements. The particularly short residence time in the jacket of the 0.5 L vessel dictated that the temperature drop along the jacket was too small to estimate the jacket duty with adequate confidence based on the experimental measurements. Of the two larger scale tests, which exhibited larger temperature drops in the thermal jacket, and thus reduced uncertainty in the experimentally determined jacket duties, the 40 L temperature profile involved a long period where the jacket inlet temperature was held constant at 40 °C. This allowed the process temperature to approach a steady state temperature, indicating a period of negligible heat accumulation in the process, $\dot{Q}_p \to 0$, coinciding with the period of maximum thermal losses. This period of negligible heat accumulation in the process and steady state heat transfer from the jacket illustrates the magnitude of the thermal losses most clearly. For these reasons, assessment of the thermal losses and the contributions of the various thermal duties will focus on these 40 L data.

4.2 Influence of thermal losses from the jacket

In order to explore the influence of the thermal jacket losses and the thermal mass of the reactor on the heating requirements of the thermoregulator, six cases will be investigated at 40 L scale. The first case considers the classical adiabatic approach with a perfectly insulated

process lid and outer jacket wall, but an elevated thermal mass to account for the thermal inertia of the reactor vessel. Case 2 considers the perfectly insulated jacket, as previously considered in Figure 4c, while cases 3-4 consider jacket-loss OHTCAs of 1,2 and 4 times the magnitude of the OHTCA for losses from the process, $(UA)_{jloss}$. Case 6 considers the effects of raising the total thermal mass of the process fluid, reactor and inserts by 50 %, thereby raising the Phi-factor from 1.08 to 1.61. The model parameters are summarized in Table 3. The predictions for (a) the evolution in process temperature, (b) the breakdown of total energy consumption, and (c) the temperature drop and thermal duty of the reactor jacket are provided in Figure 5.

Table 4: Alternative cases of heat transfer parameters used to model the 40 L experiment using eq. (3).

	$\sum_{n=1}^{N}(Mc_p)_n$ (kJ K^{-1})	Φ	$(UA)_p$ (W K^{-1})	$(UA)_{ploss}$ (W K^{-1})	$(UA)_{jloss}$ (W K^{-1})
Case 1	175	1.08	89	0	0
Case 2	175	1.08	89	3.5	0
Case 3	175	1.08	89	3.5	3.5
Case 4	175	1.08	89	3.5	7.0
Case 5	175	1.08	89	3.5	14
Case 6	263	1.61	135	5.7	0

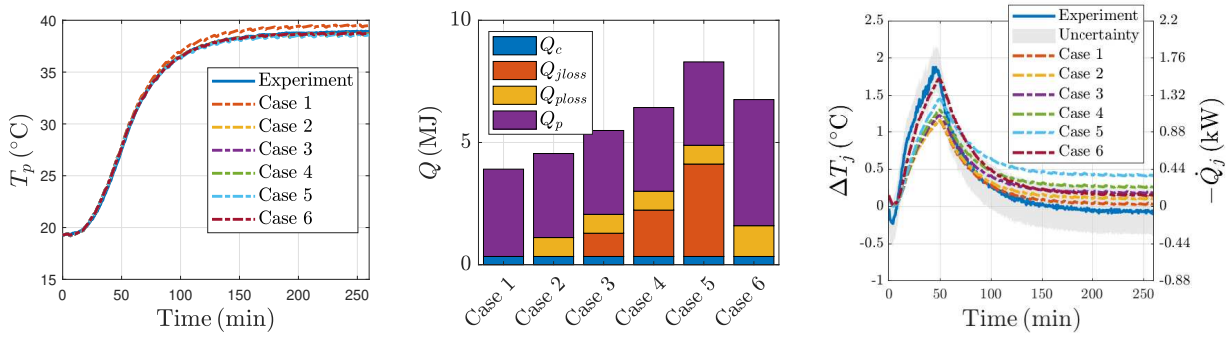

(a) (b) (c)

Figure 5: Assessment of the heat transfer model performance at 40 L scale, including (a) the evolution in process temperature, (b) the breakdown of the total energy transfer from the jacket during 260 min reactor operation, and (c) the evolution in the temperature drop along the jacket and the thermal duty of the jacket for the five cases summarized in Table 4; the uncertainty in the jacket duty profile obtained from the experimental measurements is shown as a semi-transparent grey area in (c).

With the exception of case 1, Figure 5a demonstrates that for each of the remaining cases (2-6), the predicted process temperature profiles mirror the experimental data with an accuracy similar in magnitude to the uncertainty of the experimental measurements. For the adiabatic assumption the predicted process temperature begins to exceed the experimental measurements after around 90 min, since the experimentally observed maximum process temperature is limited by thermal losses through the process lid, which are neglected in this case. The magnitude of the departure from the experimental data is in the order of 0.9 K in the adiabatic case, however this error will escalate for operations performed over a broader temperature range and when the heat transfer model is coupled with temperature sensitive reaction kinetics and significant heats of reaction.

The strong performance of each of the cases incorporating thermal losses through the process lid (cases 2-6) implies that the accurate prediction of the evolution of process temperature does not require a unique combination of heat transfer coefficients. This implies that the thermal losses from the jacket do not significantly impact the rate heat accumulation on the process side for a defined jacket inlet temperature profile. Furthermore, Figure 5b demonstrates that the jacket losses can contribute significantly to the total energy consumption without greatly influencing the rate of heat transfer to the process.

Case 5, with the greatest thermal losses from the jacket, consumes around 4 MJ of energy servicing these thermal losses from the jacket, almost doubling the total energy consumed during case 2, with the perfectly insulated jacket. Figure 5b demonstrates however that this represents an extreme case for the jacket-side losses, whereby the energy lost from the outer jacket wall exceeds the energy accumulation on the process side, which seems unrealistic given the inefficiency of free convection and thermal radiation heat transfer in air at the outer jacket wall ($\alpha_0 \sim 10\,\mathrm{W\,m^{-2}\,K^{-1}}$) in comparison with forced convection in water on the process side ($\alpha \sim 300\,\mathrm{W\,m^{-2}\,K^{-1}}$). Fortunately, uncertainty analysis of the measured temperature drop along the jacket, combined with the constraints of the energy balance, limit the range of plausible jacket-loss OHTCAs.

The uncertainty in the experimentally determined jacket temperature drop is demonstrated by the negative values recorded towards the end of the experiment, $\Delta T_j = T_{j1} - T_{j2} \approx -0.06\,\mathrm{K}$. During the final hour of data collection the process temperature is approximately steady state and thus the rate of heat accumulation in the process is negligible. Under these conditions, the rate of heat transfer from the jacket to the process is equivalent to the total thermal losses from the process, $\dot{Q}_{j-p}(t \to \infty) = \dot{Q}_{ploss} + \dot{Q}_c$, including the heat removed by the total condenser. Equally, the total jacket duty is equivalent in magnitude to the sum of all the thermal losses and the condenser duty, $-\dot{Q}_j(t \to \infty) = \dot{Q}_{jloss} + \dot{Q}_{ploss} + \dot{Q}_c$. The temperature drop along the jacket cannot be negative when $T_j(x) > T_p >> T_\infty$ and $T_p > T_{c1}$, since all three heat removal terms ($\dot{Q}_{jloss}$, $\dot{Q}_{ploss}$ and $\dot{Q}_c$) must be positive, illustrating the significance of the $\pm 0.3\,\mathrm{K}$ uncertainty in the experimental temperature measurements.

Combining uncertainty, u, analysis of the physical measurements with the constraints of the energy balance provides limiting conditions for the temperature drop along the jacket, eq. (6), and the jacket duty, eq. (7), while heat accumulation in the process is negligible:

$$\begin{aligned} u(\Delta T_j) &= \sqrt{u(T_{j1})^2 + u(T_{j2})^2} \\ \frac{\dot{Q}_{ploss} + \dot{Q}_c}{(\dot{M} c_p)_j} &\leq \Delta T_j < \Delta T_j + u(\Delta T_j) \end{aligned} \tag{6}$$

$$\begin{aligned} \frac{u(\dot{Q}_j)}{\dot{Q}_j} &= \sqrt{\left(\frac{u(\dot{M}_j)}{\dot{M}_j}\right)^2 + \left(\frac{u(\Delta T_j)}{\Delta T_j}\right)^2} \\ \dot{Q}_{ploss} + \dot{Q}_c &\leq -\dot{Q}_j < -\dot{Q}_j + u(\dot{Q}_j) \end{aligned} \tag{7}$$

For an OHTCA for process-losses of $(UA)_{ploss} = 3.5\,\mathrm{W\,K^{-1}}$, and an average condenser duty of around $0.02\,\mathrm{kW}$, the jacket duty at the end of the experiment must lay within the bounds of $0.09 \leq -\dot{Q}_j(t \to \infty) < 0.21\,\mathrm{kW}$. The two limits correspond to the cases of zero and maximum jacket-side thermal losses, and so the jacket-side thermal losses cannot exceed the breadth of this range, $\dot{Q}_{jloss} \leq 0.12\,\mathrm{kW}$. This upper-limit corresponds to a jacket-loss OHTCA of $(UA)_{jloss} \leq 5.9\,\mathrm{W\,K^{-1}}$, which indicates that the worst case for jacket-losses lies

between the scenarios modeled in cases 3 and 4.

Figure 5c, presents the temperature drop along the jacket and the jacket duty profiles for the experimental data and the five modeling scenarios. Cases 2-5 broadly model the correct shape of the jacket duty profile, but to various extents under-predict the maximum heating duty and appear to over-predict the jacket duty towards the end of the experiment. Increasing the jacket-loss OHTCA has the greatest impact towards the end of the experiment when accumulation in the process is negligible and thermal losses are at their maximum. Consequently, increasing the jacket thermal loss OHTCA has a relatively minor impact on the peak jacket duty but manifests in a gross over-estimation of the jacket duty towards the latter stages of the experiment.

Assuming the maximum possible thermal losses from the outer jacket wall, corresponding to $(UA)_{jloss} = 5.9\,\mathrm{W\,K^{-1}}$, the model still under-predicts the maximum jacket duty by around 35 %. Since the maximum jacket duty is under-predicted even with the maximum plausible thermal losses from the jacket, the heat transfer in the opposite direction, across the process-side wall, $\dot{Q}_{j-p}$, must be under-estimated, possibly indicating that the thermal mass contribution of the reactor and its contents, $\sum_{n=1}^{N}(Mc_p)_n$, is greater than anticipated (i.e. $\Phi \gg 1$).

4.3 Influence of thermal inertia

The assumed total thermal mass of the reactor system of $175\,\mathrm{kJ\,K^{-1}}$, employed by cases 1-5, includes the mass and specific heat product of (1) the process fluid, (2), the wetted portion of the reactor vessel (below the process fluid meniscus), and (3) the submerged portion of the plastic impeller. Since water has a large specific heat capacity, the process fluid contributes the bulk of the thermal mass, but the thermal contribution of the wetted vessel and inserts are by no means negligible, with the estimated Phi-factor rising from 1.08 at 40 L scale to 1.20 at 0.5 L scale. In general, the thermal contribution of the reactor walls will increase with a reduction in process scale.[18,22] However, heat will accumulate in the entire reactor

system, including the unwetted portion of the vessel and the condenser and the temperature rise in the vessel will not be homogeneous, introducing uncertainty in the proportion of the total reactor mass contributing to the thermal inertia. This uncertainty is often avoided by assuming the thermal contribution of the reactor vessel to be negligible as compared with the process fluid,[15] however the prior modeling scenarios have demonstrated that this results in an under-prediction in the magnitude of the jacket duty.

To illustrate the significance of the reactor thermal mass, case 6 considers a semi-adiabatic reactor, experiencing no thermal losses from the outer jacket wall, but with the thermal mass of the reactor and inserts increased by a factor of 1.5. Figure 5a demonstrates that the evolution of process temperature can be accurately predicted for an elevated thermal mass, providing that the OHTCAs are increased proportionately, since the rate of heat accumulation in the process scales in proportion with the thermal mass. The increased energy accumulation in the reactor system and energy lost from the process-side are shown for case 6 in Figure 5b. The condenser duty does not increase in this instance as it is estimated directly from the experimental condenser inlet and outlet temperatures. An equivalent condenser duty in each case is in fact realistic, since the amount of heat accumulation in the process fluid is identical, the increased thermal inertial manifests only in greater heat storage within the reactor vessel walls.

For each of cases 2-5, the OHTCA for heat transfer to the process is a factor of 25 greater than that for the thermal losses from the process. Consequently, scaling up the two lumped parameters proportionately will have a much greater influence on the jacket duty during the heating regime, when the driving force for heat transfer to the process, $T_j(x) - T_p$, is high, than at the steady state condition at the end of the experiment when this driving force diminishes to near zero. Scaling up the OHTCAs in unison with the thermal mass therefore has the desired effect of augmenting the magnitude of the jacket duty at its peak, without greatly influencing the steady state jacket duty towards the end of the experiment, thereby better reflecting the experimentally determined jacket duty profile in Figure 5c. Case 6 rep-

resents the only scenario which predicts the jacket duty and the process temperature profiles within their respective uncertainty limits. Thus, rather than substantial thermal losses from the outer jacket wall, the data imply substantial heat retention by the vessel (equivalent to $\approx 60\,\%$ of the heat stored by the process fluid) over the duration of experimentation, in addition to significant heat losses through the process lid. Analysis of the thermal jacket duty therefore invites the question as to whether the thermal mass contribution of the reactor components $(\Phi - 1)$ [22] may be frequently under-estimated, particularly at laboratory and pilot scales, and correspondingly whether the adiabatic assumption results in artificially low estimates for OHTCs throughout the literature.

5 Conclusions

Process fluid temperatures within laboratory to pilot scale jacketed agitated batch reactors (0.5, 5 and 40 L) were observed to depart significantly from their set temperatures during experimentation. The sluggish responsiveness of the thermoregulator feedback-control system to changes in process temperature is largely explained by the thermal inertia associated with the reactor vessel itself. Significantly enhanced reactor control, and protection against thermal runaways, can be achieved through improved characterization of the thermal inertia associated with the reactor vessel and its constituent parts as well as the thermal losses from the system.

The proposed ODE model for heat accumulation in and dissipation from the process identifies four key parameters ($\sum_{n=1}^{N}(Mc_p)_n$, $(UA)_p$, $(UA)_{ploss}$ and $(UA)_{jloss}$) which dictate the evolution of process temperature and the jacket duty. At each experimental scale an accurate prediction of process temperature required that thermal losses from the process be accounted for (i.e. $(UA)_{ploss} > 0$), however the magnitude of thermal losses from the process relative to heat accumulation in the process diminished with increased scale. Thermal losses from the outer jacket wall were not observed to significantly impact the rate of heat

accumulation in the process or the evolution of process temperature, due to the low residence times of the thermal fluid in the jacket. However, thermal losses from the outer jacket wall can appreciably increase the total jacket duty, and thus their characterisation is significant for the sizing of external heat exchangers, or thermoregulators, and for estimating operation utility costs.

Accurate prediction of the process temperature profile does not require a unique combination of heat transfer coefficients, but requires that the OHTCA for heat transfer to the process, and thermal losses from the process, are scaled according to the estimated thermal mass. Consequently, both the process temperature profile and the thermal jacket duty should be considered for the characterization of heat transfer parameters. Closer observation of the jacket duty revealed that heat accumulation within the equipment, primarily the reactor vessel walls, was significantly greater than anticipated. At 40 L scale, only when the Phi-factor, or the ratio of the total observed thermal mass of all equipment to that of the process fluid, was increased to 1.61, could both the process temperature and the jacket duty be predicted to within the uncertainty limits of the experimental measurements. Thus, heat accumulation in the reactor vessel equated to $\sim 60\,\%$ of heat accumulation in the process fluid. This potentially represents a gross limitation of widely employed classical adiabatic models, particularly at laboratory to pilot scale, since the adiabatic assumption would result in an under-estimation of the peak jacket duty by an order of around 43 % at 40 L scale. Correspondingly, this raises the potential for many OHTCs presented in the literature, derived according to the adiabatic model assumptions, to be artificially low, and may potentially be under-estimated by an order of around 50 %.

Supporting Information

- Full derivation of the non-adiabatic model for jacketed batch reactors experiencing thermal losses.

References

(1) Marroquin, G.; Luyben, W. L. Practical control studies of batch reactors using realistic mathematical models. *Chem. Eng. Sci.* **1973**, *28*, 993–1003.

(2) Bouhenchir, H.; Cabassud, M.; Le Lann, M. V. Predictive functional control for the temperature control of a chemical batch reactor. *Comput. Chem. Eng.* **2006**, *30*, 1141–1154.

(3) Crowley, T. J.; Choi, K. Y. On-line monitoring and control of a batch polymerization reactor. *J. Process Control* **1996**, *6*, 119–127.

(4) Luus, R.; Okongwu, O. N. Towards practical optimal control of batch reactors. *Chem. Eng. J.* **1999**, *75*, 1–9.

(5) Kim, H.; Lee, K. S. Reduced-heat transfer area reactor for scale-up study of batch cooling crystallization. *Ind. Eng. Chem. Res.* **2009**, *48*, 11158–11161.

(6) Fortuin, J. M.; Heiszwolf, J. J.; Bildea, C. S. Design procedure for safe operations in agitated batch reactors. *AIChE J.* **2001**, *47*, 920–928.

(7) Zhang, B.; Hou, H.; Hao, L.; Zhu, J.; Sun, Y.; Wei, H. Identification and optimization of thermally safe operating conditions for single kinetically controlled reactions with arbitrary orders in isoperibolic liquid-liquid semibatch reactors. *Chem. Eng. J.* **2019**, *375*, 121975.

(8) Papadaki, M.; Nawada, H. P. Towards improved reaction runaway assessment methods I. Simple calorimetric method of evaluation of heat transfer coefficient and reactor thermal mass. *Int. J. Chem. React. Eng.* **2003**, *1*.

(9) Martins, F. G.; Coelho, M. A. N. A new approach to evaluate the energetic efficiency of batch-jacketed reactors. *Can. J. Chem. Eng.* **2001**, *79*, 828–833.

(10) Stephanopoulos, G. *Chemical Process Control: An Introduction to Theory and Practice*; PTR Prentice Hall: Englewood Cliffs, New Jersey, 1984; Chapter 16, pp 297 – 316.

(11) Stephanopoulos, G. *Chemical Process Control: An Introduction to Theory and Practice*; PTR Prentice Hall: Englewood Cliffs, New Jersey, 1984; Chapter 22, pp 431 – 443.

(12) Jarupintusophon, P.; Le Lann, M. V.; Cabassud, M.; Casamatta, G. Realistic model-based predictive and adaptive control of batch reactor. *Comput. Chem. Eng.* **1994**, *18*, S445–S449.

(13) Niedzwiedz, M.; Laszczyk, P.; Skupin, P.; Metzger, M. Hybrid batch reactor modeling and experimental evaluation of heat transfer process. *2017 22nd International Conference on Methods and Models in Automation and Robotics, MMAR 2017* **2017**, 976–981.

(14) Bentham, E. J.; Heggs, P. J.; Mahmud, T. CFD modelling of conjugate heat transfer in a pilot-scale unbaffled stirred tank reactor with a plain jacket. *Can. J. Chem. Eng.* **2019**, *97*, 573–585.

(15) Heggs, P. D., P. J.; Hills *Heat Exchange Engineering*; Honeysuckle International Publications: Bradford, England, 1994; Vol. 4; Chapter 14.

(16) Luus, R. Optimal control of batch reactors by iterative dynamic programming. *J. Process Control* **1994**, *4*, 218–226.

(17) Krämer, S.; Gesthuisen, R. Simultaneous estimation of the heat of reaction and the heat transfer coefficient by calorimetry: Estimation problems due to model simplification and high jacket flow rates - Theoretical development. *Chem. Eng. Sci.* **2005**, *60*, 4233–4248.

(18) Johnson, M.; Heggs, P. J.; Mahmud, T. Assessment of overall heat transfer coefficient models to predict the performance of laboratory-scale jacketed batch reactors. *Org. Process Res. Dev.* **2016**, *20*, 204–214.

(19) Chilton, T. H.; Drew, T. B.; Jebens, R. H. Heat Transfer Coefficients in Agitated Vessels. *Ind. Eng. Chem.* **1944**, *36*, 510–516.

(20) Mohan, P.; Nicholas Emery, A.; Al-Hassan, T. Review heat transfer to Newtonian fluids in mechanically agitated vessels. *Exp. Therm. Fluid Sci.* **1992**, *5*, 861–883.

(21) Malone, R. J. Sizing external heat exchangers for batch reactors. *Chem. Eng.* **1980**, 95–101.

(22) Waldram, S. Toll manufacturing: Rapid assessment of reactor relief systems for exothermic batch reactions. *Process Saf. Environ. Prot. Trans. Inst. Chem. Eng., Part B* **1994**, *72*, 149–156.

(23) Leung, J. Simplified vent sizing equations for emergency relief requirements in reactors and storage vessels. *AIChE Journal* **1986**, *32*, 1622–1634.

(24) Patel, N.; Nease, J.; Aumi, S.; Ewaschuk, C.; Luo, J.; Mhaskar, P. Integrating Data-Driven Modeling with First-Principles Knowledge. *Ind. Eng. Chem. Res.* **2020**, *59*, 5103–5113.

(25) Esposito, M.; Sayer, C.; De Araújo, P. H. H. In-Line Monitoring of Emulsion Polymerization Reactions Combining Heat Flow and Heat Balance Calorimetry. *Macromol. React. Eng* **2010**, *4*, 682–690.

(26) Erdoğan, S.; Alpbaz, M.; Karagöz, A. R. The effect of operational conditions on the performance of batch polymerization reactor control. *Chem. Eng. J.* **2002**, *86*, 259–268.

(27) De Dietrich Process Systems GmbH., *QVF SUPRA-Line: The component system 04 Vessels*; 2020; p 14.

Table of contents graphic